Multi-Functional Heat Pulse Probe for the Simultaneous Measurement of Soil Water Content, Solute Concentration, and Heat Transport Parameters

Y. Mori, J. W. Hopmans,* A. P. Mortensen, and G. J. Kluitenberg

ABSTRACT

Water, solute, and heat transport processes in soils are mutually interdependent as each includes convective water flow and each transport mechanism is partly controlled by fluid saturation, pore geometry, temperature, and other soil environmental conditions. Therefore, their measurement in approximately identical measurement locations and volume is essential for understanding transport phenomena in soils. We introduce a 2.7-cm-diameter multi-functional heat pulse probe (MFHPP), which consists of a single central heater, four thermistors, and four electrodes (Wenner array) that together are incorporated in six 1.27-mm-o.d. stainless-steel tubes. The bulk soil thermal properties and volumetric water content of Tottori Dune sand were determined from the measurement of the temperature response of all four thermistor sensors after application of an 8-s heat pulse by the heater sensor. Simultaneously with the temperature measurements, the bulk soil electrical conductivity (EC_b) was measured using the Wenner array, from which soil solution concentration (EC_w) can be obtained after calibration. All measurements were taken during multistep outflow experiments, which also allowed estimation of the soil's hydraulic properties. We demonstrated that the MFHPP can effectively measure volumetric water content, thermal properties, and EC_b, and can be used to indirectly estimate soil water fluxes at rates larger than 0.7 m d^{-1} in the sand.

The vadose zone in general moderates the impact of soil contamination to groundwater and air quality as determined by soil processes such as water flow and chemical and heat transport. All of these processes are interrelated, as each is controlled by pore-scale transport mechanisms and are dependent on convective water flow. Specifically, dissolved chemical constituents are transported in the vadose zone by convective water flow, so that chemical fate is partly controlled by the water regime. Soil thermal properties control the soil's thermal regime, thereby affecting water flow and chemical transport. Moreover, thermal and chemical transport properties are highly dependent on the degree of water saturation. Thus, to improve our understanding of soil environmental processes and their control of water and air quality, it is important to evaluate the coupling mechanisms and their relevance to environmental issues. Since both soil water content and temperature generally change with time, both diurnally as well as at larger time scales, it is important that the various coupled transport processes are measured simultaneously.

In addition to being variable in time, soil transport properties and processes are known to be highly variable in space. Because of the inherent soil spatial heterogeneity, the outcome of a soil measurement is dependent on measurement volume. The scale dependency of soil properties and their relation to vadose zone flow and transport processes have precluded a unifying concept of water flow and chemical transport across spatial scales, from the microscopic pore scale to the macroscopic local scale (Hopmans et al., 2002b). Therefore, it is essential to estimate soil properties at the same location, using approximately equal measurement volumes. Hence, the justification of the proposed MFHPP is to ensure that the different measurement types are conducted within identical soil volumes, minimizing soil heterogeneity effects and providing more accurate measurements of soil physical properties for environmental monitoring.

The proposed MFHPP originates from the dual-probe heat-pulse (DPHP) method introduced by Campbell et al. (1991). The DPHP method was experimentally tested by Bristow et al. (1993, 1994b), whereas measurement errors were analyzed by Kluitenberg et al. (1993, 1995). Additional work (Bristow et al., 1993) showed that the DPHP method provides an alternative means to measure soil water content, in addition to the measurement of the soil's thermal properties. The successful application of the DPHP method has been demonstrated for both laboratory (Bristow et al., 1994b; Bilskie et al., 1998; Basinger et al., 2003) and field soils (Tarara and Ham, 1997). By incorporating time domain reflectometry (TDR) into the DPHP method, Noborio et al. (1996) and Ren et al. (1999) conducted simultaneous measurement of soil thermal properties, water content, and electrical conductivity (EC). The so-called thermo-TDR probe was successfully demonstrated by Ochsner et al. (2001). Bristow et al. (2001) demonstrated that a DPHP with two additional sensors for EC_b measurements allows for the simultaneous estimation of soil solution concentration.

In an independent study by Ren et al. (2000), it was shown that the temperature responses of the upstream and downstream sensors of a three-sensor heat pulse probe (HPP) can be used to indirectly estimate the water flux density. Hopmans et al. (2002a) demonstrated successfully an inverse technique by which thermal properties, water content, and water fluxes could be estimated from temperature measurements by including both conductive and convective heat transport in the two-dimen-

Y. Mori, Faculty of Life and Environmental Sciences, Shimane University, Shimane, Japan; J.W. Hopmans, Hydrology, Dep. of Land, Air and Water Resources, University of California, Davis, CA 95616; A.P. Mortensen, Geological Institute, Copenhagen University, Copenhagen, Denmark; and G.J. Kluitenberg, Dep. of Agronomy, Kansas State University, Manhattan, KS 66506. Received 25 Mar. 2003. Special Section—Advances in Measurement and Monitoring Methods. *Corresponding author (jwhopmans@ucdavis.edu).

Published in Vadose Zone Journal 2:561–571 (2003).

677 S. Segoe Rd., Madison, WI 53711 USA

Abbreviations: DPHP, dual-probe heat-pulse; DSC, differential scanning calorimetry; EC, electrical conductivity; HPP, heat pulse probe; MFHPP, multi-functional heat pulse probe; TDR, time domain reflectometry.

sional heat flow equation while accounting for dispersive heat transport caused by pore water flow variations. The MFHPP proposed herein was developed for the simultaneous analysis and measurement of water flow, solute, and thermal transport properties. Whereas we are not completely confident that the measurement volumes of all sensors are identical, their inclusion within a single probe would certainly limit the effect of spatial variations within the probe's measurement volume, when compared with measurements with separate sensors that must be installed at different locations.

In this study, we developed a small prototype of a MFHPP with six sensors, a heater, four thermistors, and four Wenner-array electrodes. The primary objective was to evaluate the accuracy of the probe, regarding its application to determine the water content dependency of the soil's volumetric heat capacity and thermal heat diffusivity, using the transient temperature responses of each of the four thermistors during multi-step outflow experiments. Our secondary objective was to demonstrate the potential application of using the MFHPP to measure EC_b and water fluxes, simultaneously with the soil water content and thermal property measurements.

THEORY

Thermal Properties (C, κ, and λ) and Volumetric Water Content (θ)

Thermal property estimation using the HPP method is based on a solution of the heat conduction equation for an infinite line heat source in a homogeneous and isotropic medium that is initially at uniform temperature. For a heat pulse of duration t_0 (s), the solution for the temperature change, ΔT (K) at a distance r (m) from the line heat source is given by (de Vries, 1952; Kluitenberg et al., 1993; Bristow et al., 1994a):

$$\Delta T(r,t) = \frac{q'}{4\pi C\kappa}\left[\mathrm{Ei}\left(\frac{-r^2}{4\kappa(t - t_0)}\right) - \mathrm{Ei}\left(\frac{-r^2}{4\kappa t}\right)\right]; \quad t > t_0 \qquad [1]$$

where q' is the energy input per unit length of heater per unit time (W m^{-1}), C and κ are the soil's volumetric heat capacity (J m^{-3} K^{-1}) and thermal diffusivity (m^2 s^{-1}), respectively, and $-\mathrm{Ei}(-x)$ is the exponential integral function with argument x (Abramowitz and Stegun, 1972). The thermal conductivity of the bulk soil, λ (W m^{-1} K^{-1}), is determined from the product of C and κ. For HPP measurements, r represents the spacing between heater and temperature sensor. Whereas q' and t can be measured with high accuracy, measurement of r is more problematic. Therefore, it is recommended to determine an effective separation distance, r_{eff}, by fitting Eq. [1] to temperature measurements of a medium with known thermal properties. However, as pointed out by Kluitenberg et al. (1995), solution of Eq. [1] is highly sensitive to variations in sensor spacing. Insertion of the HPP into a different medium after calibration might change sensor spacing, thereby affecting the solution and fitted thermal property values. Moreover, as pointed out in Basinger et al. (2003), contact resistance between the sensors and the surrounding medium might vary, thereby affecting the fitted r value. Alternatively, it would be beneficial to measure r in situ, so that r_{eff} is determined for the soil to be studied.

Once C is estimated from Eq. [1], the volumetric water content, θ (m^3 m^{-3}), can be determined from (de Vries, 1963; Campbell, 1985):

$$C = \rho_b c_s + C_w\theta \qquad [2]$$

assuming that the specific heat value of air can be ignored and the specific heat values of the solid phase and water are available. In Eq. [2], ρ denotes the material density (kg m^{-3}); c is the specific heat (J kg^{-1} K^{-1}); $C_w = \rho_w c_w$; and subscripts "b", "s", and "w" denote bulk soil, solid phase, and water, respectively.

Electrical Conductivity (EC_b, EC_w)

In addition to the heater and thermistor sensors, the MFHPP includes a four-electrode sensor as described by Inoue et al. (2000). It consists of four parallel electrodes that constitute a Wenner-array configuration, by which the bulk electrical resistance of the medium between the inner electrodes of the array can be determined. After sensor-specific calibration, by which the bulk electrical conductivity of the medium, EC_b, is related to the measured electrical resistance, the EC_w of a soil solution can be related to EC_b by calibration using soil solutions of known concentrations. Rhoades et al. (1976) proposed the expression

$$EC_b = \theta\tau(\theta)EC_w + EC_s \qquad [3a]$$

$$\tau(\theta) = a\theta + b, \qquad [3b]$$

which defines the control of θ, a water content dependent tortuosity term $\tau(\theta)$, and the soil solid surface conductivity (EC_s) on the bulk soil electrical conductivity. Rearranging Eq. [3] yields

$$\frac{EC_b}{EC_w} = a\theta^2 + b\theta + \frac{EC_s}{EC_w} \qquad [4]$$

After calibration, Eq. [4] provides a means to estimate the soil solution conductivity, EC_w, from measurements of θ . The calibration consists of fitting Eq. [4] to measured EC_b and θ data for known EC_w, yielding values for coefficients a and b, and the soil surface conductivity, EC_s. For the sandy material used in this study, the value of EC_s was assumed zero.

Darcy Water Flux (J_w)

Equation [1] is valid if heat transport occurs by conduction only. Ren et al. (2000) presented an analytical solution for the heat equation that includes convective heat transport, where the convective heat flux density, J_h, is defined as

$$J_h = \frac{C_w J_w}{C} \qquad [5]$$

assuming that the soil's solid and fluid phases are in thermal equilibrium. They also showed that measurement of the difference in temperature responses between the upstream and downstream temperature sensor of a three-sensor HPP provides the additional necessary information to estimate the water flux density, J_w. The complex mathematical relationship proposed by Ren et al. (2000) was later replaced with the much simpler approximation (Wang et al., 2002):

$$J_w \approx \frac{2C\kappa}{C_w(r_d + r_u)}\ln\left(\frac{T_d}{T_u}\right) \qquad [6]$$

where the subscripts "u" and "d" denote the upstream and downstream sensors, respectively. This approximation becomes an equality in the limit as $t \to \infty$ (Wang et al., 2002). As pointed out by Hopmans et al. (2002a), this expression may not apply for high water fluxes where thermal dispersion becomes significant, as determined by the Keith–Jirka–Jan number that quantifies the ratio of thermal dispersivity and conductivity.

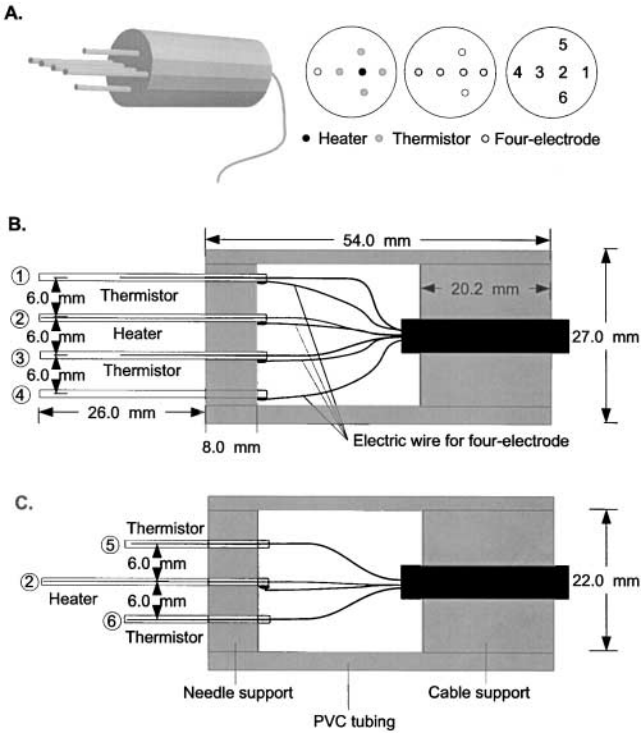

Fig. 1. Design of multi-functional heat pulse probe (MFHPP).

Multistep Outflow Method (θ, h_m, K)

The measurements of soil thermal properties, water content, soil solution conductivity, and water flux can be combined with multistep outflow experiments (van Dam et al. 1994; Eching et al., 1994; Hopmans et al., 2002c) to estimate the soil water retention, $\theta(h_m)$, and unsaturated hydraulic conductivity, $K(\theta)$, functions. Soil water retention data were fitted with the van Genuchten model (1980):

$$S_e = \left(1 + |\alpha h_m|^n\right)^{-m} \quad [7a]$$

$$S_e = \left(\theta - \theta_r\right)/\left(\theta_s - \theta_r\right) \quad [7b]$$

whereas the unsaturated hydraulic conductivity was described by the pore-size distribution model of Mualem (1976) to yield (van Genuchten, 1980)

$$K(\theta) = K_s S_e^l \left[1 - \left(1 - S_e^{1/m}\right)^m\right]^2 \quad [8]$$

In Eq. [7] and [8], S_e denotes the effective saturation ($0 \leq S_e \leq 1$); θ_r ($m^3\ m^{-3}$) is the residual water content; θ_s ($m^3\ m^{-3}$) is the saturated water content; K_s ($m\ s^{-1}$) is the fitted saturated hydraulic conductivity; and α (cm^{-1}), n, m ($m = 1 - 1/n$), and l (assumed to be 0.5) are empirical parameters.

MATERIALS AND METHODS

Multi-Functional Heat Pulse Probe

A schematic of the MFHPP prototype is presented in Fig. 1. It consists of six parallel sensors with a spacing of approximately 6 mm between them. Sensor 2 serves as a both a heater and electrode. Temperature responses are measured by four thermistors (Sensors 1, 3, 5, and 6) at approximately equal radial distances from the heater sensor. Sensors 1, 2, 3, and 4 comprise the four-electrode Wenner array for bulk soil EC measurements (Fig.1b).

All sensors were constructed from 1.27-mm-o.d. and 0.84-mm-i.d. (18-gauge) stainless-steel tubing (Small Parts, Inc., Miami Lakes, FL) with a single flared end. Sensors 5 and 6 were only one-half the length of the other sensors (Fig. 1c) to minimize potential deflection of those sensors during insertion of the MFHPP. This was possible as they were not part of the Wenner array.

The heater was constructed by threading enameled wire (79-μm-diam., 205 $\Omega\ m^{-1}$, Nichrome 80 alloy; Pelican Wire Co., Naples, FL) through the tubing four times, resulting in two loops with a resistance of 820 $\Omega\ m^{-1}$. The temperature sensors were constructed by placing a thermistor (0.46-mm-diam., 10 kΩ at 25°C, 0.004°C precision as measured at 20°C; Model 10K3MCD1, Betatherm Corp., Shrewsbury, MA) in the center of the sensors. The four Wenner-array sensors were wired for current (Sensors 1 and 4) and voltage measurements (Sensors 2 and 3). All sensors were filled with Omegabond 101 epoxy (Omega Engineering, Stamford, CT), which has a relatively high thermal conductivity and is a good electrical insulator. Sensors were secured into predrilled holes in a 22.0-mm-diam. and 8.0-mm-thick PVC plug. All 14 lead wires were soldered to 14 corresponding wires of a 20-wire shielded multiconductor cable (Model 9542, 24AWG, Belden, Richmond, IN). The multiconductor cable was held in place by another 20-mm-long PVC plug. Omegabond epoxy was injected into the cavity of the MFHPP to ensure electrical insulation of all wires and that the probe was waterproof.

Data Acquisition

Heating and temperature and conductivity measurements were controlled by a CR10 datalogger (Campbell Scientific Inc., Logan, UT) and three AM416 multiplexers (Campbell Scientific), powered by a 12-V AC-DC converter. Both the thermistor and four-electrode measurements were conducted using four-wire half-bridge circuits, with a 5-kΩ bridge resistor (0.1% tolerance; Vishay Resistors, Malvern, PA), installed at the CR10. Current was determined from measurement of the voltage drop across the reference resistor. The desired heat input to the heater sensor was attained by applying 12 V to the heater sensor for approximately 8 s. Cumulative heat input was measured using a 1-Ω current-sensing resistor (0.1% tolerance; Model VPR5, Campbell Scientific) in the heater circuit of the CR10. Resistance measurements of all thermistors were converted to temperature by using the Steinhart-Hart equation (BetaTHERM, 1994). From calorimetric temperature measurements in a stirred water–ice mixture, the accuracy of the $\Delta T(t)$ measurements was estimated to be about 0.01°C.

Estimation of EC_w was accomplished by measuring EC_b with the MFHPP Wenner array. The electrical current across the four electrodes of the Wenner array is determined from an applied voltage (V_1) across the two outer sensors, using a reference resistor, R_f (10 Ω, 5% tolerance), that was placed at the CR10, in series with the voltage measurement. Subsequently, the bulk soil resistance is computed from the ratio of the electrical current and the measured voltage difference (V_2) between the two inner sensors, which is inversely proportional to EC_b, according to

$$EC_b = c\frac{V_2}{V_1} \quad [9]$$

where c is the cell constant of the Wenner array. Its magnitude depends on R_f and is a function of the sensor geometry. It was determined by calibration using eight different KCl solutions with conductivities in the range of 0 to 13 $dS\ m^{-1}$, as measured with an EC meter (Model 115plus, Thermo Orion, Beverly, MA). The R^2 value of the fitted linear regression line was 0.999, resulting in a cell constant value of 0.0051.

Table 1. Physical properties of washed Tottori Dune sand and thermal properties of water.

Soil	Tottori Dune sand
ρ_b, kg m^{-3}	1630
K_s, m s^{-1}†	2.4 × 10^{-4}
θ_s, m^3 m^{-3}	0.371
c_s at 20 and 30°C, J kg^{-1} K^{-1}	795.0 and 814.6
ρ_w at 20 and 30°C, kg m^{-3}	998.2 and 995.7
c_w at 20 and 30°C, J kg^{-1} K^{-1}	4181.6 and 4178.2
C_w at 20 and 30°C, kJ m^{-3} K^{-1}	4174 and 4160
κ_w at 20 and 30°C, m^2 s^{-1}	1.4 and 1.5 × 10^{-7}

† K_s denotes the measured saturated hydraulic conductivity.

The datalogger was programmed so that EC_b and the initial temperature for all thermistors were measured first, followed by heating of the heating sensor and the subsequent simultaneous measurement of the temperature responses of all four thermistors for 180 s at 1-s intervals. Measurement of EC_b was done before the heating because of the temperature dependency of electrical conductivity. Measurement cycles were repeated at 15-min intervals or longer, ensuring that all heat of the previous heating cycle had dissipated.

Soil Description

Experiments were conducted with a Tottori Dune sand (Inoue et al., 2000) because it allows for rapid saturation and drainage across a wide water content range. The sand was washed to eliminate potential clogging of the porous membrane by organic matter and/or clay-sized particles. Physical properties are listed in Table 1. Specific heat was measured by differential scanning calorimetry (DSC; Kay and Goit, 1975) across a temperature range of 0 to 120°C. Three samples were run, with a CV of 2%. Before the DSC measurement, the sand was oven dried, and vacuum was applied. During the specific heat measurements, the soil sample was kept in a dry nitrogen environment. Over the temperature range of 20 to 30°C, the temperature coefficient of c_s was about 1.9 J kg^{-1} K^{-1} per °C (Fig. 2), which is larger than reported by Kluitenberg (2002).

MFHPP Calibration and Multistep Outflow Experiments

The effective separation distance (r_{eff}) for all four thermistor sensors was first determined from HPP measurements in 4 g L^{-1} agar solutions (Campbell et al., 1991). The possibility of a salinity effect on the HPP measurements was explored by dissolving $CaCl_2$ in separate agar solutions, but no effect was detected. The r_{eff} value for each thermistor sensor was determined by fitting the measured heat pulse response to Eq. [1], using known values of the water's volumetric heat capacity (4174 kJ m^{-3} K) and thermal diffusivity (1.436 × 10^{-7} m^2 s^{-1}). Optimizations were conducted by fitting r to the temperature response curves. Values of r_{eff} were also determined after installation of the MFHPP in the Tottori dune sand. This in situ calibration was done after full saturation of the Tottori sand with water, by CO_2 flushing, and required the use of κ as an additional fitting parameter. Independent measurements of the bulk density, specific heat, and saturated water content (Table 1) were used to estimate C.

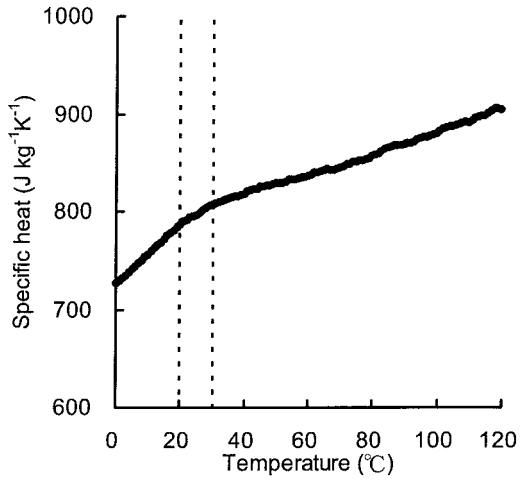

Fig. 2. Experimentally determined temperature dependency of specific heat of the Tottori sand.

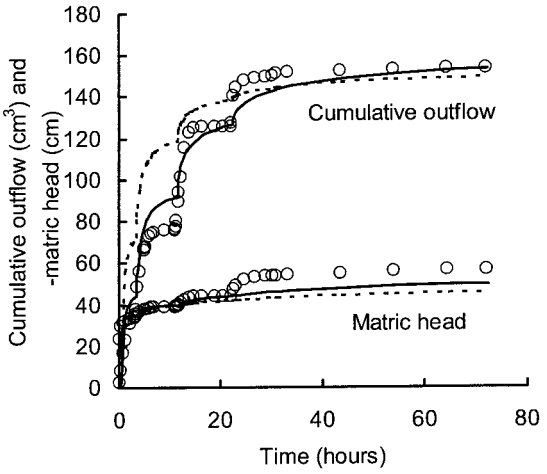

Fig. 3. Comparison of measured with optimized matric head and cumulative outflow for the 0.06 *M* solution.

The Tottori sand was dry packed at a dry bulk density of 1.63 Mg m^{-3} into a 10-cm-long and 7.9-cm-i.d. Plexiglas flow cell. A porous nylon membrane (pore size 20 μm; Osmonics R22SP14225, GE Osmonics Labstore, Minnetonka, MN) glued onto a stainless perforated plate ensured hydraulic continuity between the drained flow cell and the drainage outlet. The flow cell was saturated with a 0.015 $CaCl_2$ solution (0.03 *M* Cl^-) after CO_2 was introduced, to achieve full saturation. A miniature tensiometer (Tuli et al., 2001) and a single MFHPP were installed horizontally in the center of the flow cell. Throughout the experimental period, laboratory temperature was held constant within a range of 18 to 21°C.

The MFHPP measurements were conducted during periods of hydraulic equilibrium of a single multi-step outflow experiment, using suction increments of 10, 20, 30, 40, 50, and 100 cm. Cumulative drainage and tensiometer readings were collected at 1-min intervals during outflow experiments that lasted about 3 d (Fig. 3). After the last suction step of 100 cm, CO_2 was reintroduced and the flow cell was resaturated with a 0.06 *M* Cl^- solution. Similarly, the multi-step outflow experiment and resaturation procedure was repeated with a 0.10 *M* Cl^- solution. After resaturation with a new solution, the flow cell was flushed with at least two pore volumes of the new solution. Leachate conductivity was monitored to ensure complete flushing. Following this wetting procedure, all three outflow experiments were conducted with the same flow cell at approximately equal saturation values.

Results of parameter fitting of the soil water retention curve of the coarse-textured Tottori sand quickly revealed the enormous sensitivity of h_m to θ. Specifically, within the h_m range from −20 to −40 cm, the sand's volumetric water content changed from 0.37 to about 0.1 m^3 m^{-3}. Because the retention curve is highly nonlinear within this range, the volumetric water

content in the center of the cell is not necessarily equal to the flow cell's average water content (Dane and Hopmans, 2002). Consequently, it was difficult to ascertain whether the MFHPP measurements in the center of the flow cell were accurate. It was therefore decided to repeat some of the outflow experiments after sectioning the Plexiglas flow cell into five rings with heights of 1.5, 1.5, 4.0, 1.5, and 1.5 cm, with the central 4-cm-high ring containing the horizontally installed MFHPP. Outflow experiments were repeated four times to achieve final applied suctions of 30, 35, 40, and 50 cm, solely to compare MFHPP water content estimates with gravimetric water content measurements of the central ring at hydraulic equilibrium. Additional comparisons were obtained from separate measurements in glass jars. For this purpose, the sand was mixed with predetermined amounts of water in plastic bags. The mixtures were packed in glass jars at the required dry bulk density of 1.63 Mg m^{-3}. After thermal equilibrium with the laboratory environment, the MFHPP was vertically inserted from the surface down, and measurements were conducted to estimate volumetric water content. Values of r_{eff} were determined from measurements at saturation. Independent water content data were obtained from oven drying of the top 2.6 cm of soil.

Parameter Fitting

Data collected from the multistep outflow experiments consisted of transient matric head and outflow measurements. The SFOPT code (Tuli et al., 2001) was used to optimize the soil hydraulic parameters α, n, θ_r, and K_s, while minimizing the residuals of the measured and simulated cumulative drainage (Q) and soil water matric head (h_m). Data collected from the HPP measurements consisted of transient temperature measurements. Temperature data were fit to Eq. [1] using Solver in Excel (Wraith and Or, 1998) as the nonlinear optimization algorithm while minimizing the residuals between measured and predicted $\Delta T(t)$ curves, given a priori values for q' and r_{eff}, as described by Welch et al. (1996) and Bristow et al. (1995).

RESULTS AND DISCUSSION

Multistep Outflow and Soil Hydraulic Properties

Optimization for each of the three outflow experiments resulted in three sets of soil hydraulic parameters. Average estimated hydraulic parameters values were $\alpha = 0.026$ cm^{-1}, $n = 10.378$, $\theta_r = 0.0312$ cm^3 cm^{-3}, and $K_s = 3.33$ cm h^{-1}, whereas θ_s was fixed to its average measured value of 0.371 cm^3 cm^{-3}. The resulting optimized soil water matric head and cumulative outflow (solid lines) are compared with their respective measurements (open circles) in Fig. 3 for the 0.06 M experiment. The RMSE values between measured and fitted matric head and cumulative outflow were 4.1 cm and 9.9 cm^3, respectively. Similar or better matching of measured with optimized data was obtained for the other two outflow experiments. The MFHPP measurements were conducted in the various stages of near-zero flow at pseudo hydraulic equilibrium. Although Kluitenberg and Heitman (2002) showed that transient water flow conditions and resulting convective heat flow do not necessarily affect the HPP measurements, we decided not to compromise the HPP measurements by the presence of convective heat flow.

The resulting optimized hydraulic functions for all

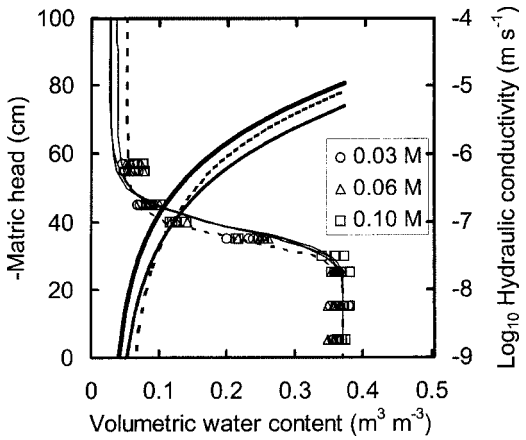

Fig. 4. Optimized soil hydraulic functions. The symbols correspond with measured soil water retention data at the hydraulic equilibrium stages of Fig. 3, using the multi-functional heat pulse probe (MFHPP) and tensiometer data.

three outflow experiments are presented by the partly overlapping solid curves in Fig. 4. The various data points correspond with the water content–matric head data in the center of the flow cell, as measured with the MFHPP and miniature tensiometer for hydraulic equilibrium at each pressure step. For each of the three solutions, the multiple data points correspond with water content values as estimated from the individual thermistor sensors. After averaging, these water content data were included in the objective function, resulting in optimized functions represented by the dashed lines in Fig. 3 and 4 for the 0.06 M solution outflow experiment. Corresponding optimized parameter values were $\alpha = 0.0288$ cm^{-1}, $n = 12.179$, $\theta_r = 0.054$ cm^3 cm^{-3}, and $K_s = 3.01$ cm h^{-1}. The differences in optimized functions and their comparison with the independent data show the difficulties in obtaining accurate soil hydraulic data for this coarse-textured sandy material, because of the large sensitivity of h_m to θ. The relatively wide range in the measured θ values for the three separate outflow experiments is also attributed to this high sensitivity. The measured soil water retention data in Fig. 4 illustrate yet another important point; that is, although the final applied suction was 100 cm, the measured pseudo-equilibrium soil water matric head in the center of the soil remained at about −57 cm. The reason for this deviation between expected and measured soil water matric potentials was presented by Eching and Hopmans (1993) and more recently by Gee et al. (2002). Particularly in sandy soils, the unsaturated hydraulic conductivity at increasing suction becomes so low that it prevents the soil from attaining hydraulic equilibrium.

Electrical Conductivity Probe Calibration of MFHPP

Relationships between water content and EC_b for the three different soil solution concentrations are shown in Fig. 5. The individual data points were obtained at the hydraulic equilibrium stages of near-zero drainage flow in Fig. 3. The EC_b values were determined from the Wenner array calibration curve in Eq. [9]. The volu-

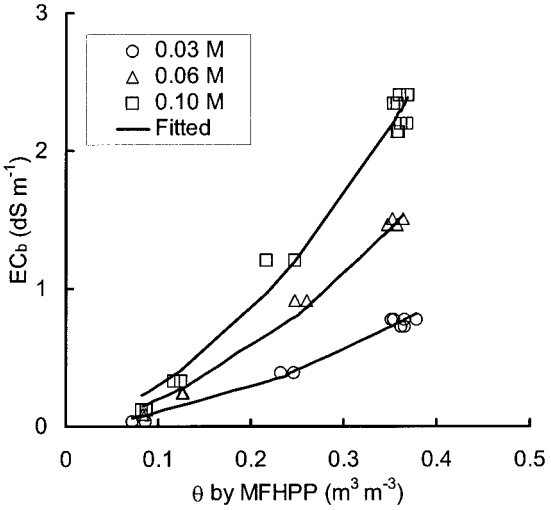

Fig. 5. Calibration of the Wenner array of the multi-functional heat pulse probe (MFHPP) for the Tottori Dune sand.

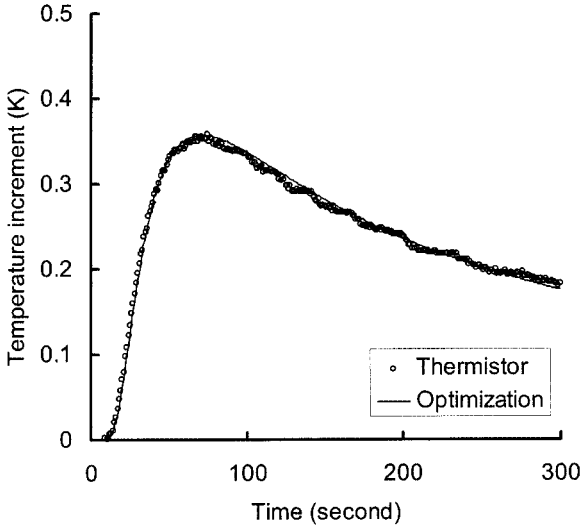

Fig. 6. Measured and optimized temperature response for the estimation of r_{eff} in agar solution.

metric water content values were determined from the fitting of the thermistor responses of Sensors 1 and 3 of the Wenner array of the MFHPP to Eq. [1], using the sensor-specific r_{eff} values that were estimated from the in situ calibrations. The presented curves in Fig. 5 were obtained by fitting Eq. [4] to the experimental data, assuming that EC_s is zero. Fitted values for a and b were 1.330 and 0.167, respectively, with an R^2 value of 0.994. Regression coefficient values agreed well with corresponding values reported by Inoue et al. (2000) for the Tottori Dune sand. However, we reluctantly eliminated the water content data values smaller than 0.10 cm^3 cm^{-3} because their inclusion tended to result in a negative intercept. There are several reasons to suspect the accuracy of the water content or EC measurements at the lower water content values. First, as will be shown below, the uncertainty of the water content measurements increases as θ decreases. Also, some overestimation might be the result of disregarding the temperature effect of bulk soil thermal properties (Kay and Goit, 1975; Hopmans and Dane, 1986). Although the maximum temperature rise at the thermistors was typically in the range 0.5 to 1.5°C, the maximum temperature rise is greater in the region between the thermistor and the heater, increasing exponentially with proximity to the heater. Alternatively, the deviations at low water content might be caused by underestimation of the EC_b measurements because of reduced contact between the two inner sensors of the Wenner array and the surrounding bulk soil. In all, we found that the EC_b measurements using the Wenner array of the MFHPP can be used for the volumetric water content range of values >0.10 cm^3 cm^{-3}. We conclude that within this valid range of the EC calibration, the Wenner-array measurements can provide soil solution concentration data for coarse-textured soils, provided accurate water content values can be obtained from MFHPP measurements. This result is consistent with results presented by Inoue et al. (2000) and Bristow et al. (2001).

Sensor Spacing Calibration of MFHPP (r_{eff})

The thermal response of one of the thermistor sensors in the agar solution is presented in Fig. 6. The optimized r_{eff} values for all sensors were obtained from known values of the volumetric heat capacity and heat diffusivity of water at 20°C (first two columns in Table 2). The RMSE values were generally in the range of 0.0055 to 0.0166 K. The large heat capacity of the agar solution caused extensive tailing of the heat pulse response, necessitating measurements of temperature for at least 5 min after application of the heat pulse. Since both C_w and κ_w were assumed known, only r_{eff} was fitted to Eq. [1]. Values for the respective sensors (Fig. 1) varied between 0.5634 and 0.5875 cm, with a maximum difference between effective sensor spacing of about 0.25 mm. We note that these differences are likely caused by errors introduced by the assumptions of Eq. [1], in addition to true variations in sensor spacing. Assumptions that were violated came about from (i) application of Eq. [1] to a finite heat source whereas the solution is for an infinite heat source and (ii) fabrication of heater and thermistor sensors, such as variations in position of the thermistor within the steel tubing and differences in thermal properties of the sensors and epoxy filler relative to the surrounding soil (Kluitenberg et al., 1995).

Fitted values for r_{eff} and κ_w after saturation of the Tottori sand was done by pooling the temperature responses for all three solution concentrations and saturated measurements (0 and 10 cm suction) for each thermistor sensor separately. Thus, the resulting six temperature responses combined were fitted to Eq. [1], of

Table 2. Calibration of the effective needle spacings, r_{eff}.

	Agar at 20°C	Saturated soil at 20°C		Saturated soil at 30°C	
Sensor	r_{eff}	r_{eff}	κ	r_{eff}	κ
	m		$\times 10^{-7}$ $m^2 s^{-1}$	m	$\times 10^{-7}$ $m^2 s^{-1}$
1	0.005652	0.005701	6.2	0.005688	6.1
3	0.005875	0.005721	5.8	0.005699	5.8
5	0.005634	0.005965	6.4	0.005943	6.3
6	0.005859	0.005956	7.0	0.005934	7.0

which the results are presented in the third and fourth columns of Table 2. The MFHPP was installed in the flow cell, before soil packing, and sensor spacing calibration was done for the fully saturated sand. We might expect different effective values for primarily two reasons. First, although the sensors of the HPP are quite rigid, some flexing may occur after repeated use, thereby changing the spacings. Second, one may suppose that the contact resistance between the thermistor sensors and agar solution is different than that of a heterogeneous porous media with three different phases (Basinger et al., 2003). Both effects were likely small in our experiments. Values for r_{eff} ranged between 0.5701 and 0.5965 cm. The range of these values is similar to the agar calibration; however, the average values are slightly larger, as would be the case if the contact resistance increases. Despite the fact that the sand was uniformly packed and saturated, the variability of the estimated soil thermal diffusivity between the four thermistor sensors was quite large, ranging from 5.8 to 7.02 $\times 10^{-7}$ m^2 s^{-1}, corresponding to a CV of about 8%. In part, this may be caused by slight inhomogeneities in porosity and associated saturated water content, as well as variations between sensor geometry and associated thermal properties. Also, the large variance of thermal diffusivity may be explained by differences in contact resistance between the sensors, thereby causing variations in the time response of the heat signals. In contrast, C is mostly controlled by the maximum temperature change, which is much less affected by contact resistance. From multiple HPP measurements at saturation, we determined that instrument precision was about 1% for the C measurements and about 2% for the κ measurements.

Table 2 also lists values for r_{eff} assuming that the bulk soil temperature was 30°C instead of the assumed 20°C, taking into consideration a possible temperature affect as caused by soil heating during the thermistor measurements. As the results show, the temperature effect on the sensor spacings was very small, with slightly lower values of r_{eff} at the elevated temperature.

Soil Thermal Properties (C, κ, and λ)

Examples of thermal responses at hydraulic equilibrium for the 0.10 M solution experiment for 120 s are presented in Fig. 7. Whereas the symbols represent the measured data, the lines were fitted using Eq. [1] with C and κ as fitting parameters. In general the fit is excellent with typical RMSE values of about 0.0149 K; however, one must realize that the fitted thermal properties are effective properties with values that correct for contact resistance and other violations of using Eq. [1]. Bristow et al. (1995) recommended exclusion of the data at longer times, because deviations from the underlying theory are expected to occur in the tails of the temperature response curve. As expected, the change in soil temperature decreases as the water content increases and the temperature peak is maximal at the lowest presented water content. The resulting thermal diffusivity and thermal conductivity data as a function of water content from these optimizations for all three outflow

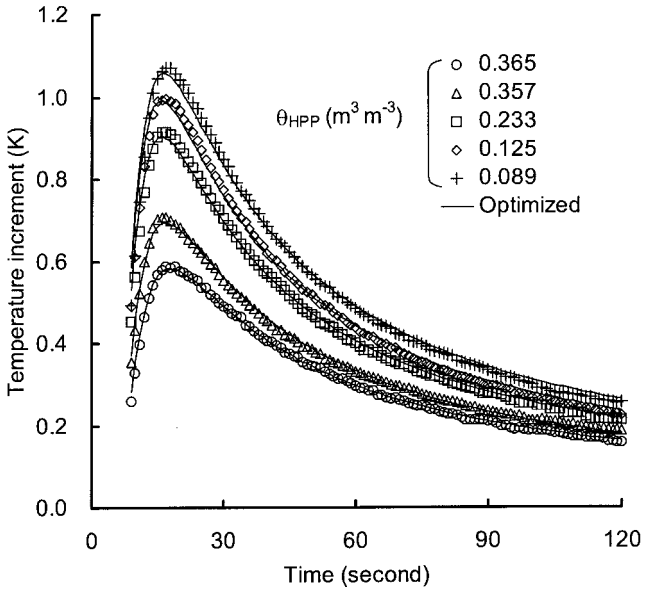

Fig. 7. Thermal responses at various soil water content values for the Tottori sand.

experiments are shown in Fig. 8. As expected, there was no clear difference in thermal properties between the three salt solutions. The optimized thermal properties are compared with the data of Bristow et al. (2001), who applied the Campbell (1985) model for a sandy soil (98% sand) with about equal bulk density of 1520 kg m^{-3}, and with the experimental data of Hopmans and Dane (1986) for a sandy loam soil with a bulk density of 1560 kg m^{-3}. Our MFHPP data agreed very well with the independent measurements of Hopmans and Dane (1986); however, there were some differences with the Campbell (1985) model. As pointed out by Bristow et al. (2001), model prediction of the soil thermal properties is a function of soil mineralogy. In addition, Table 3 presents the mean data (from four thermistor sensors) and CV as computed from the three outflow experiments. When pooling the results for all three outflow experiments, the general uncertainty (CV) in C, κ, and λ across the full range of water content is between 0.5 and 2%.

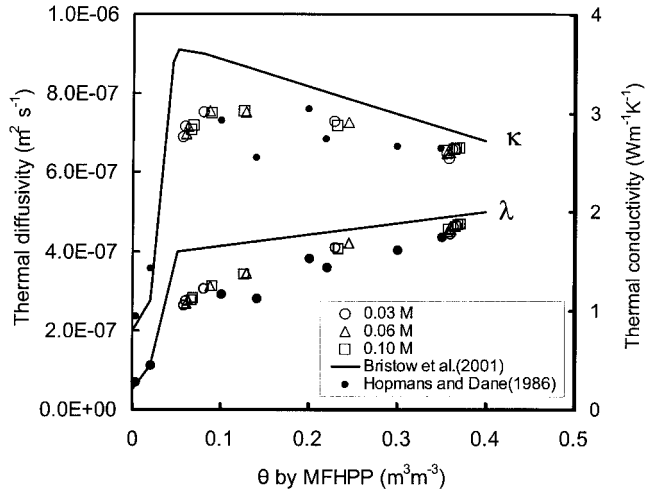

Fig. 8. Estimated average soil thermal properties for the three solution concentrations compared with independent data.

Table 3. Results of multi-functional heat pulse probe (MFHPP) measurements.†

Suction	*C*	*CV*	κ	*CV*	λ	*CV*	θ	*CV*	EC_b/EC_w	*CV*
cm	kJ m^{-3} K^{-1}	%	× 10^{-7} m^2 s^{-1}	%	W m^{-1} K^{-1}	%	m^3 m^{-3}	%		%
0	2803.8	0.9	6.5	2.0	1.8	2.7	0.36	1.6	0.23	3.3
10	2817.9	1.1	6.6	1.2	1.9	2.2	0.37	1.9	0.24	3.9
20	2809.2	0.4	6.6	0.7	1.8	0.9	0.36	0.7	0.23	3.3
30	2279.0	1.5	7.3	0.7	1.7	1.8	0.24	3.5	0.13	8.9
40	1652.0	1.3	7.5	0.2	1.2	1.2	0.09	5.8	0.01	6.1
50	1558.6	1.1	7.2	0.2	1.1	1.3	0.06	6.8	0.003	46.8
100	1549.7	1.2	7.0	1.2	1.1	2.4	0.06	7.4	0.001	145.2

† Average of four thermistor sensors.

Volumetric Water Content (θ)

Using Eq. [2], water content was estimated from the MFHPP measurements of the draining soil. As the results in Table 3 show, the CV of the water content measurements increase as the water content decreases, with CV values larger than 5% at θ values smaller than 0.10 m^3 m^{-3}. As indicated above, because of the high nonlinearity of the retention curve, the local HPP water content measurements cannot be directly compared with average water content values in the flow cell as inferred from outflow measurements. Instead, to determine the accuracy of the HPP measurements, Fig. 9 compares water content measurements for the sectioned flow cell (open circles) and the independent measurements in the glass jars (solid dots) with gravimetric water content data determined from oven drying. Rather than using the individual water content values for each thermistor sensor, we present the average water content measurements, resulting in a combined number of 26 data points. Using linear regression, the fitted intercept and slope were 0.0046 and 0.9644, respectively, with R^2 and RMSE values of 0.985 and 0.014 m^3 m^{-3}, respectively. Alternatively, when using the estimated water content values of each thermistor sensor (104 data points), the RMSE value increased to 0.0299 m^3 m^{-3}, similar to the corresponding value reported by Basinger et al. (2003). We conclude that the uncertainty of the water content measurements decreased significantly when averaged for the four thermistor sensors of the MFHPP. The uncertainty may be due to measurement error, but could also be partially caused by soil spatial variations within the measurement volume of the MFHPP. In contrast to other studies (e.g., Basinger et al., 2003), our MFHPP measurements did not overestimate volumetric water content in the low water content range.

Figure 10 compares measured with simulated water content data for the 0.06 *M* multistep outflow experiment after establishment of hydraulic equilibrium for suction values of 30, 35, 40, and 50 cm. The measured water content data (open symbols) were determined from oven drying of the sectioned flow cell. The two different simulated water content profiles (solid and dashed lines) were computed using the two sets of optimized soil hydraulic functions (corresponding solid and dashed lines) in Fig. 4. In addition, Figure 10 includes the MFHPP measurements in the center of the draining flow cell (solid symbols). Whereas there is generally an acceptable agreement between measured and simulated water content values for all but the bottom compartment of the flow cell, significant deviations of about 0.05 m^3 m^{-3} were determined for the bottom of the flow cell. It is likely that some water entrapment occurred there, resulting in larger measured water content values than using the solution of the unsaturated water flow equation. Similar results were reported by Wildenschild et al. (2001) and Mortensen et al. (2001), who explained the larger water content values by air blockage of water flow above the porous membrane.

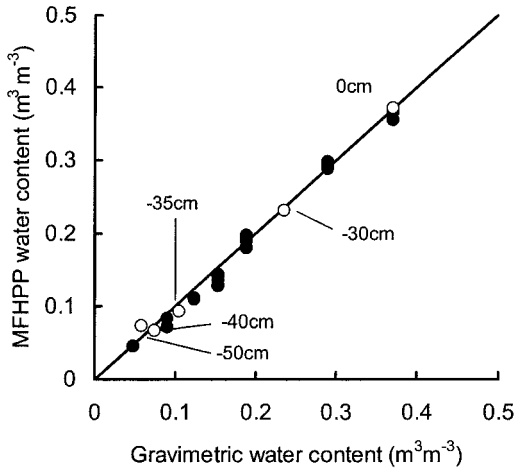

Fig. 9. Comparison of θ measurements with multi-functional heat pulse probe (MFHPP) and gravimetric method. Solid circles indicate glass jar experiments; open circles denote the multistep outflow experiments.

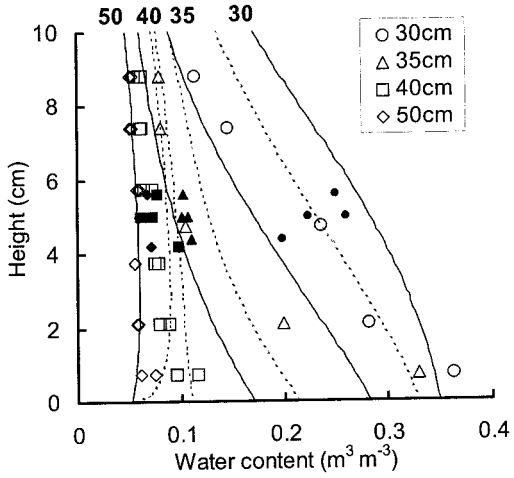

Fig. 10. Variation of θ with height in flow cell as determined from gravimetric (open symbols), SFOPT simulations (solid and dashed lines), and MFHPP data (solid circles) for the indicated suction values.

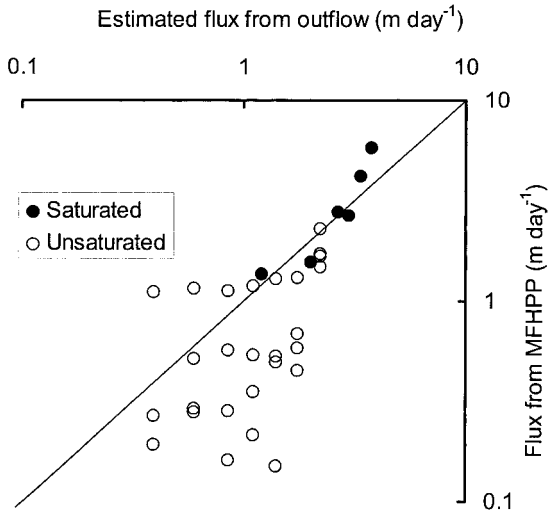

Fig. 11. Comparison of measured (multi-functional heat pulse probe [MFHPP]) with simulated water flux (SFOPT) values in the center of the flow cell for various multistep outflow experiments.

Finally, we were also interested in the possible temperature effect on the water content measurements. Using the 20°C calibration results of the effective sensor spacing, we computed the water content values from Eq. [2] for one of the outflow experiments (0.06 M), using specific heat and water density values of 30°C (Table 1). Differences in estimated water content were $<1\%$ ($m^3\ m^{-3}$) across the whole water content range, with θ values at 30°C always smaller than at 20°C.

Water Flux Density (J_w)

Using Eq. [6], the water flux density during drainage of the unsaturated sand was estimated from the ratio of the downstream and upstream temperatures, for times (t) of 50 to 60 s. For the water flux estimations, only the MFHPP measurements during the first 30 min of the 30-cm suction step of the multistep outflow experiments with the sectioned flow cell were used. Since the flux estimations were determined from MFHPP measurements in the center of the flow cell, these fluxes cannot be directly compared with the measured drainage data of Fig. 3. Instead, water fluxes were computed from the SFOPT simulations using the optimized soil hydraulic functions (solid lines in Fig. 4). The results of this comparison are presented in Fig. 11 by the open circles. A comparison at higher flow velocities was possible by conducting a separate saturated steady-state flow experiment (solid circles in Fig. 11), achieving a range of flux densities by changing the total head gradient across the flow cell. In all, the combined experiments allowed a comparison for water fluxes in the range of 0.15 to 4.5 m d^{-1}. Although both fluxes are close for values >1.0 m d^{-1}, fluxes as estimated from the MFHPP measurements significantly underestimated the simulated water fluxes as calculated with SFOPT for fluxes smaller than 1.0 m d^{-1}. We note that complications are expected to occur at the lower water flow velocities for various reasons. First, the MFHPP measurements are limited by the resolution of the temperature measurements. As was already demonstrated by Ren et al. (2000), one cannot expect accurate water flux measurements for flow velocities <0.06 m d^{-1}, when the accuracy of the temperature measurements is about 0.01°C. However, discrepancies were significant at flow velocities in the range of 0.1 to 1.0 m d^{-1}. Second, the simplified analytical solution of Wang et al. (2002) only considers the total distance between the upstream and downstream thermistors, but does not explicitly account for differences in spacing between the heater and the two thermistor sensors. Moreover, the analytical solution does not account for possible water content variations between the upstream and downstream temperature sensors. Third, as for the thermal diffusivity measurements, we expect that uncertainties in the estimated heat pulse velocity are caused by variations in construction of the upstream and downstream thermistor sensors. Fourth, we noticed that the simulated water flux values are extremely sensitive to the soil hydraulic functions of the Tottori sand of this study. Results for the water flow velocities >0.7 m d^{-1}, however, show very good agreement between the two types of water flux estimates. This supports the presented data for the sandy soil by Ren et al. (2000), but we expect that corrections for thermal dispersion are required for finer-textured soils at the higher water flux densities. In a future study, we plan to improve the water flux density estimations in the low flow range using inverse solution of the transient combined water flow and heat transport equation by minimizing residuals of simulated and measured temperature responses, as proposed in Hopmans et al. (2002a).

CONCLUSIONS

The results obtained with the MFHPP sensor demonstrate the advantages of simultaneous measurement of water flow, solute, and heat transport properties within an approximately equal measurement volume. After calibration of the radial spacing between the heater and thermistor sensors of the MFHPP, accurate measurements of the volumetric heat capacity, thermal conductivity and diffusivity, and volumetric water content can be obtained. In addition, when combined with a multistep outflow experiment, soil water retention and unsaturated hydraulic conductivity functions were estimated in concert with the MFHPP measurements. However, our experimental results also showed some limitations. First, water content data can only be obtained when having a priori knowledge of the soil's specific heat. Second, the Wenner array estimations of soil solution EC appear to be valid only for volumetric water content values >0.10 $m^3\ m^{-3}$. Third, thermal diffusivity and water content estimations vary widely among the four thermistor sensors of the MFHPP. We hypothesize that these variations are largely caused by differences in sensor fabrication and by nonideal thermal properties of the filling epoxy and stainless-steel tubing resulting in temperature response variations between the sensors. However, accurate estimates of both thermal properties and water content were obtained when their values for

the four thermistor sensors were averaged. Finally, additional research is needed to improve water flux estimations at flow rates smaller than 0.7 m d^{-1} and to accurately determine the measurement volumes and spatial sensitivity of the EC and temperature response measurements.

ACKNOWLEDGMENTS

Authors are grateful to Dr. Keith Bristow of CSIRO Land and Water, Australia, for allowing us to examine their prototype model of the DPHP. We acknowledge the contribution of Dr. Alexandra Navrotsky, of the University of California Davis, for the specific heat measurements of the Tottori Dune sand in her laboratory. We thank Prof. Mitsuhiro Inoue, Arid Land Research Center, Japan, for his shipment of the Tottori Dune sand. We appreciate the assistance of Jason Ritter, Campbell Scientific Inc., for his valuable advice on the datalogger programming. This work was partially supported by the Japan Society for the Promotion of Science (2001–2003) and AES project CA-D*-LAW-7117-H.

REFERENCES

Abramowitz, M., and I. Stegun. 1972. Handbook of mathematical functions. Dover Publ., New York.

Basinger, J.M., G.J. Kluitenberg, J.M. Ham, J.M. Frank, P.L. Barner, and M.B. Kirkham. 2003. Laboratory evaluation of the dual-probe heat-pulse method for measuring soil water content. Available at www.vadosezonejournal.org. Vadose Zone J. 2:389–399.

BetaTHERM Corp. 1994. BetaTHERM NTC thermistor products 1994–1995 catalog. BetaTHERM Corp., Shrewsbury, MA.

Bilskie, J.R., R. Horton, and K.L. Bristow. 1998. Test of a dual-probe heat-pulse method for determining thermal properties of porous materials. Soil Sci. 163:346–355.

Bristow, K.L., J.R. Bilskie, G.J. Kluitenberg, and R. Horton. 1995. Comparison of technique for extracting soil thermal properties from dual-probe heat-pulse data. Soil Sci. 160:1–7.

Bristow, K.L., G.S. Campbell, and C. Calissendorff. 1993. Test of a heat-pulse probe for measuring changes in soil water content. Soil Sci. Soc. Am. J. 57:930–934.

Bristow, K.L., G.J. Kluitenberg, C.J. Goding, and T.S. Fitzgerald. 2001. A small multi-sensor probe for measuring soil thermal properties, water content and electrical conductivity. Comput. Electron. Agric. 31:265–280.

Bristow, K.L., G.J. Kluitenberg, and R. Horton. 1994a. Measurement of soil thermal properties with a dual-probe heat-pulse technique. Soil Sci. Soc. Am. J. 58:1288–1294.

Bristow, K.L., R.D. White, and G.J. Kluitenberg. 1994b. Comparison of single and dual probes for measuring soil thermal properties with transient heating. Aust. J. Soil Res. 32:447–464.

Campbell, G.S. 1985. Soil physics with BASIC—Transport models for soil-plant systems. Elsevier, New York.

Campbell, G.S., C. Calissendorff, and J.H. Williams. 1991. Probe for measuring soil specific heat using a heat-pulse method. Soil Sci. Soc. Am. J. 55:291–293.

Dane, J.H., and J.W. Hopmans. 2002. Water retention and storage: Computational corrections. p. 714–715. *In* J.H. Dane and G.C. Topp (ed.) Methods of soil analysis. Part 4. SSSA Book Ser. 5. SSSA, Madison, WI.

de Vries, D.A. 1952. A nonstationary method for determining thermal conductivity of soil in situ. Soil Sci. 73:83–89.

de Vries, D.A. 1963. Thermal properties of soils. p. 210–235. *In* W.R. van Wijk (ed.) Physics of plant environment. North Holland Publishing Company, Amsterdam.

Eching, S.O., and J.W. Hopmans. 1993. Optimization of hydraulic functions from transient outflow and soil water pressure data. Soil Sci. Soc. Am. J. 57:1167–1175.

Eching, S.O., J.W. Hopmans, and O. Wendroth. 1994. Unsaturated hydraulic conductivity from transient multi-step outflow and soil water pressure data. Soil Sci. Soc. Am. J. 58:687–695.

Gee, G.W., A.L. Ward, Z.F. Zhang, G.S. Campbell, and J. Mathison. 2002. The influence of hydraulic nonequilibrium on pressure plate data. Available at www.vadosezonejournal.org. Vadose Zone J. 1:172–178.

Hopmans, J.W., K.L. Bristow, and J. Simunek. 2002a. Indirect estimation of soil thermal properties and water flux from heat pulse measurements: Geometry and dispersion effects. Water Resour. Res. 38 DOI:10.1029/2000WR000071.

Hopmans, J.W., and J.H. Dane. 1986. Thermal conductivity of two porous media as a function of water content, temperature, and density. Soil Sci. 142:187–195.

Hopmans, J.W., D.R. Nielsen, and K.L. Bristow. 2002b. How useful are small-scale soil hydraulic property measurements for large-scale vadose zone modeling. p. 247–258. *In* D. Smiles et al. (ed.) Heat and mass transfer in the natural environment. The Philip Volume. Geophysical Monogr. Ser. 129. AGU, Washington, DC.

Hopmans, J.W., J. Simunek, N. Romano, and W. Durner. 2002c. Simultaneous determination of water transmission and retention properties. Inverse methods. p. 963–1008. *In* J.H. Dane and G.C. Topp (ed.) Methods of soil analysis. Part 4. SSSA Book Ser. 5. SSSA, Madison, WI.

Inoue, M., J. Šimunek, S. Shiozawa, and J.W. Hopmans. 2000. Simultaneous estimation of soil hydraulic and solute transport parameters from transient infiltration experiments. Adv. Water Resour. 23:677–688.

Kay, B.D., and J.B. Goit. 1975. Temperature dependent specific heats of dry soil materials. Can. Geotech. J. 12:209–212.

Kluitenberg, G.J. 2002. Heat capacity and specific heat. p. 1201–1226. *In* J.H. Dane and G.C. Topp (ed.) Methods of soil analysis. Part 4. SSSA Book Ser. 5. SSSA, Madison, WI.

Kluitenberg, G.J., K.L. Bristow, and B.S. Das. 1995. Error analysis of the heat pulse method for measuring soil heat capacity, diffusivity and conductivity. Soil Sci. Soc. Am. J. 59:719–726.

Kluitenberg, G.J., J.M. Ham, and K.L. Bristow. 1993. Error analysis of the heat pulse method for measuring soil volumetric heat capacity. Soil Sci. Soc. Am. J. 57:1444–1451.

Kluitenberg, G.J., and J.L. Heitman. 2002. Effect of forced convection on soil water content measurement with the dual-probe heat-pulse method. p. 275–283. *In* D. Smiles et al. (ed.) Heat and mass transfer in the natural environment. The Philip Volume. Geophysical Monogr. Ser. 129. AGU, Washington, DC.

Mortensen, A.P., R.J. Glass, K. Hollenbeck, and K.H. Jensen. 2001. Visualization of microscale phase displacement processes in retention and outflow experiments: Nonuniqueness of unsaturated flow properties. Water Resour. Res. 37:1627–1640.

Mualem, Y. 1976. A new model for predicting the hydraulic conductivity of unsaturated porous media. Water Resour. Res. 12:513–522.

Noborio, K., K.J. McInnes, and J.L. Heilman. 1996. Measurements of soil water content, heat capacity, and thermal conductivity with a single TDR probe. Soil Sci. 161:22–28.

Ochsner, T.E., R. Horton, and T. Ren. 2001. Simultaneous water content, air-filled porosity, and bulk density measurements with thermal-time domain reflectometry. Soil Sci. Soc. Am. J. 65:1618–1622.

Ren, T., G.J. Kluitenberg, and R. Horton. 2000. Determining soil water flux and pore water velocity by a heat pulse technique. Soil Sci. Soc. Am. J. 64:552–560.

Ren, T., K. Noborio, and R. Horton. 1999. Measuring soil water content, electrical conductivity, and thermal properties with a thermo-time domain reflectometry probe. Soil Sci. Soc. Am. J. 63: 450–457.

Rhoades, J.D., P.A.C. Raats, and R.J. Prather. 1976. Effects of liquid-phase electrical conductivity, water content, and surface conductivity on bulk soil electrical conductivity. Soil Sci. Soc. Am. J. 40: 651–655.

Tarara, J.M., and J.M. Ham. 1997. Measuring soil water content in the laboratory and field with dual-probe heat-capacity sensors. Agron. J. 89:535–542.

Tuli, A., M.A. Denton, J.W. Hopmans, T. Harter, and J.L. MacIntyre. 2001. Multi-step outflow experiment: From soil preparation to parameter estimation. Land, Air and Water Resources Rep. 100037. University of California, Davis.

van Dam, J.C., J.N.M. Stricker, and P. Droogers. 1994. Inverse method

to determine soil hydraulic functions from multistep outflow experiments. Soil Sci. Soc. Am. J. 58:647–652.
van Genuchten, M.Th. 1980. A closed-form equation for predicting the hydraulic conductivity of unsaturated soils. Soil Sci. Soc. Am. J. 44:892–898.
Wang, Q. J, T.E. Ochsner, and R. Horton. 2002. Mathematical analysis of heat pulse signals for soil water flux determination. Water Resour. Res. 38 DOI: 10.1029/2001WR001089.
Welch, S.M., G.J. Kluitenberg, and K.L. Bristow. 1996. Rapid numerical estimation of soil thermal properties for a broad class of heat-pulse emitter geometries. Measur. Sci. Technol. 7:932–938.
Wildenschild, D., J.W. Hopmans, and J. Simunek. 2001. Flow rate dependence of soil hydraulic characteristics. Soil Sci. Soc. Am. J. 65:35–48.
Wraith, J.M., and D. Or. 1998. Nonlinear parameter estimation using spreadsheet software. J. Nat. Resour. Life Sci. Educ. 27:13–19.